Pergamon

Journal of Structural Geology, Vol. 17, No. 8, pp. 1111 to 1124, 1995

0191-8141/95 $9.50 + 0.00

0191-8141(95)00002-X

Tectonic versus mineralogical contribution to the magnetic fabrics of epimetamorphic slaty rocks: an example from the Ardennes Massif (France–Belgium)

PHILIPPE ROBION and DOMINIQUE FRIZON DE LAMOTTE

Université de Cergy-Pontoise, Structure des Matériaux Géologiques (CNRS URA 1369, antenne de Cergy), 95033 Cergy-Pontoise Cédex, France

and

CATHERINE KISSEL

Centre des Faibles Radioactivités (CNRS-CEA), Domaine du CNRS, Av. de la terrasse, 91 198 Gif-sur-Yvette Cédex, France

and

CHARLES AUBOURG

Université de Cergy-Pontoise, Structure des Matériaux Géologiques (CNRS URA 1369, antenne de Cergy), 95033 Cergy-Pontoise Cédex, France

(*Received* 7 *June* 1994; *accepted in revised form* 12 *December* 1994)

Abstract—The discrimination of the respective contribution of strain and mineralogy of the bulk Anisotropy of low field Magnetic Susceptibility (AMS) of rocks is addressed by a study of the Ardennes Variscan Thrust Belt. Unmetamorphosed to low-medium-grade rocks in the study area define a succession of magnetic parageneses: hematite + maghemite (?), hematite + maghemite (?) + magnetite, magnetite + pyrrhotite. A direct control of the magnetic mineralogy on the magnitude of AMS axes is shown. In addition, in all cases, the interpretation of the directions of AMS axes as kinematic indicators also applies to these rocks. We show a progressive change in shearing direction from the south of the Rocroi massif, where the nappe transport is N-directed; in the north, the vergence changes to northwestward.

INTRODUCTION

Anisotropy of low field Magnetic Susceptibility (AMS) study is a fast and precise petrofabric tool that is particularly effective in apparently undeformed regions (Kissel *et al.* 1986, Lee *et al.* 1990) or in fold-thrust belts (Averbuch *et al.* 1992, Averbuch *et al.* 1993) where standard petrofabric techniques are inadequate or inefficient. In more deformed areas, the development of magnetic fabric studies is hindered by the changes in rock mineralogy. These changes, linked to metamorphism, occur even in a zone of very low-grade and inhibit any quantitative interpretation (Rochette & Lamarche 1986, Borradaile 1987).

On the other hand, in such domains structural markers (cleavage, lineation, etc.) give direct deformation about finite strain and can make magnetic fabric analysis useless. However, numerous regions of very low or low-grade metamorphism show ubiquitous and regular slaty cleavage affecting rocks over large areas but no other tectonic markers. Previous work shows that changes in magnetic fabric occur within such rocks even if they appear similar in the field. The tectonic interpretation of these variations are not straightforward: in some cases they can be related to variations in tectonic regime (e.g. a coaxial vs no-coaxial tectonic regime; Aubourg *et al.* 1991), but in others they seem to be connected only to changes in magnetic mineralogy (Housen & Van der Pluijm 1991).

The purpose of this paper is to discriminate between the influence of tectonic strain and magnetic mineralogy. We will present data from the Variscan Thrust Belt in the Ardennes (France, Belgium). This largely Hercynian deformed zone exhibits rocks of various metamorphic grade from unmetamorphosed to medium-grade affected by an ubiquitous cleavage. A previous study conducted in a part of the area we investigated has been already published (Rathore & Hugon 1987).

GEOLOGICAL SETTING AND SAMPLING

The France–Belgium Ardennes Variscan domain is a zone of large-scale overthrusting (Fourmarier 1913, Kaisin 1936). Surface geology, shallow and deep structures of this orogenic belt are relatively well constrained by detailed mapping, extensive mining-related work in Carboniferous coal-fields bore-holes (Bouroz 1950) and

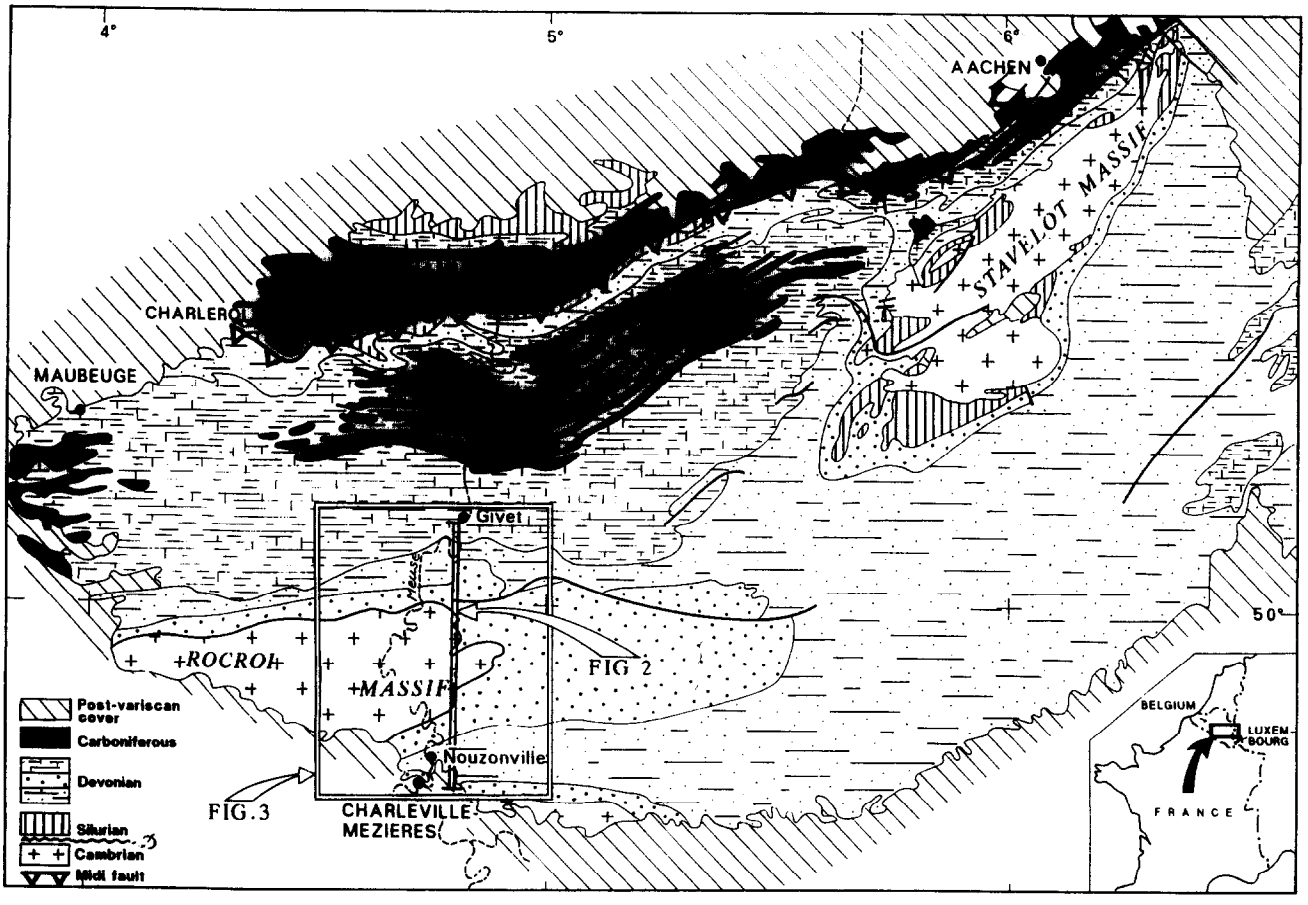

Fig. 1. Sketch map of the Ardennes fold and thrust belt, with location of the studied area (Figs. 2 and 3).

a deep seismic reflection profile (Cazes *et al.* 1985). Recent syntheses give a present-day interpretation of the sedimentary and tectonic evolution of this belt using modern thrust-tectonic concepts (Meilliez 1989, Meilliez & Mansy 1990, Meilliez 1991).

The Ardennes massif can be divided into two main zones, the Brabant parautochthonous units (including the 'Namur syncline' in the north) and the Ardennes allochthonous units in the south. These two zones are separated by a major thrust zone called the Midi fault (Fig. 1). The sedimentary pile involved in the tectonic wedge forming the Ardennes allochthonous units comprises a pre-Devonian basement unconformably overlain by Devono-Carboniferous formations.

The pre-Devonian rocks consist mainly of Cambrian to lower Ordovician quartzites, sandstones and shales (Beugnies 1963). They crop out mainly in the Rocroi and Stavelot massifs forming wide culminations of Variscan age. Across the first massif, the deep Meuse valley provides a good natural section of the belt from Nouzonville to Givet (Fig. 2). The Rocroi massif exhibits numerous recumbent folds which are unconformably overlaid with Devonian units. The significance of this unconformity, called the Ardennes Unconformity (Waterlot 1937), is still a matter of debate (Hugon 1982, Delvaux de Fenffe & Laduron 1984). However in the field, two points are clear: (1) rocks situated above and beneath the unconformity display apparently similar strain (see below); and (2) the unconformity is a sedimentary contact (Beugnies 1963; Meillez *et al.* 1994) and not a ductile shear plane as suggested by Le Gall (1992).

North of the Rocroi anticline, the Upper Palaeozoic series consist of conglomerates, sandstones and shales of Early Devonian to Eifelian age overlaid with limestones of Givetian age. South of the Rocroi anticline, the Devonian comprises essentially slaty rocks interpreted as basinal metasedimentary rocks.

The tectonic style of the Devonian rocks from north to south of the Rocroi massif is different. North of the Rocroi massif, it consists of gently overturned concentric folds. Within argillaceous rocks, the axial plane of these folds is marked by a S-dipping cleavage. South of the Rocroi massif, in the Neufchateau syncline, the rocks are involved in syn-cleavage recumbent folding. The tectonic transport direction is northward.

Changes in the tectonic style occur in the central part of the Rocroi massif and are related to the development of a metamorphic dome along the southern boundary of the Rocroi massif (Fig. 1). As the early porphyroblast are prekinematic, Meilliez (1991) considers these metamorphic domes as the effects of a Devonian crustal stretching. However, the development of new minerals within the Variscan cleavage and post-kinematic mineral growth show that the thermal dome, located on the south of the present-day Rocroi massif, persisted from Devonian to Carboniferous.

In order to study the internal deformation of the rocks using AMS, a total of 411 oriented cores were drilled in

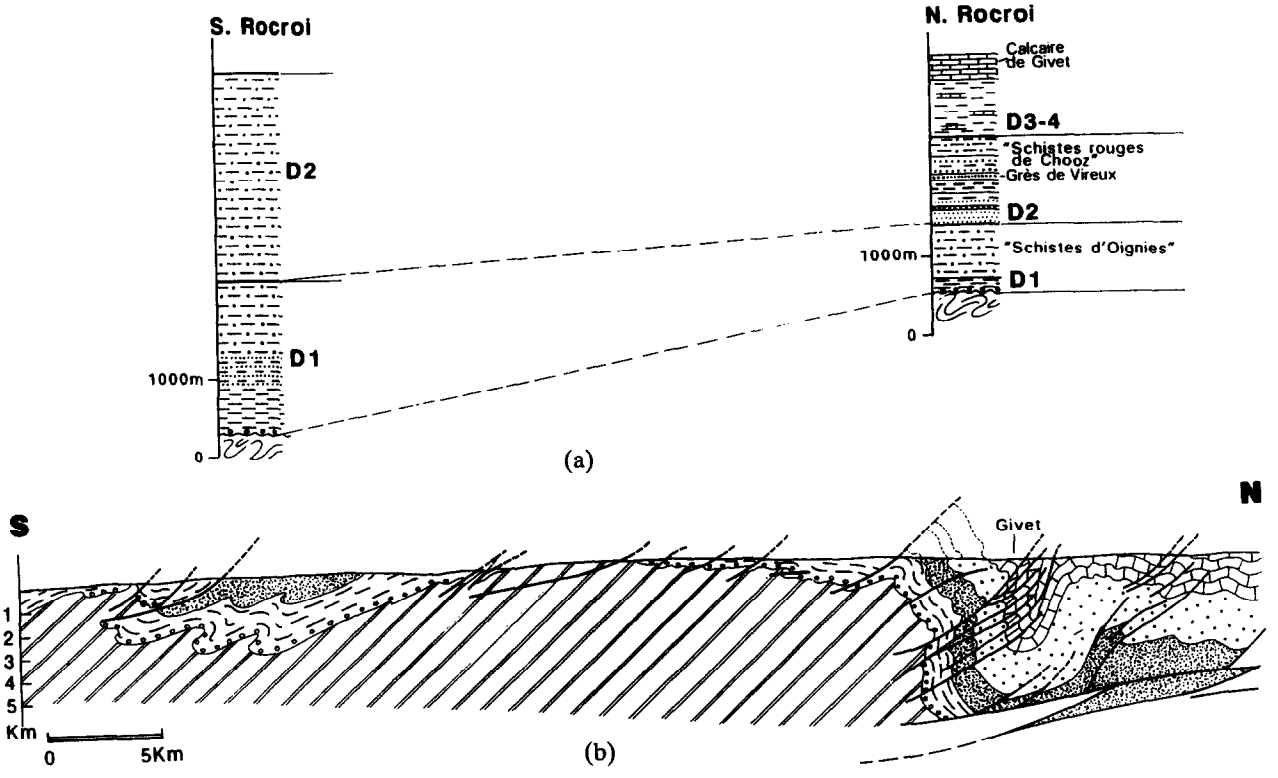

Fig. 2. (a) Stratigraphic sections north and south of the Rocroi massif from Meillez *et al.* (1992). D_{1-2}: Lower Devonian; D_{3-4}: Middle Devonian. (b) Schematic cross-section of the studied area (from Raoult 1988).

36 sites. Their geographical distribution is shown in the Fig. 3.

Five sites were sampled in the so-called 'schistes rouges de Chooz' of Emsian age. In this area Devonian rocks are involved in a large asymmetric kink fold (the Vireux fold), from a vertical to slightly overturned forelimb and a subhorizontal back limb. Sites 2, 8 and 16 were sampled in the vertical limb and sites 3 and 28 in the horizontal limb.

The second set of sites has been sampled in the Gedinnian formation called 'Schistes d'Oignies'. These sites are located either north of the Rocroi massif or south of it, distributed along the Semoy river oriented E–W in this area.

The third set of sites 18, 32 to 40 was sampled in the Cambrian shells of the Rocroi massif. They are located near the Meuse river along a general N–S section.

LABORATORY ANALYSES AND RESULTS

Analysis of magnetic fabrics

In a low magnetic field ($4.5\ 10^{-5}$ T), anisotropic behaviour of the magnetic susceptibility is described by a second-order tensor. It can be visualized as an ellipsoid characterized by three principal axes ($K_1 \geq K_2 \geq K_3$) corresponding to the eigenvectors of the tensor and describing the statistical preferential alignment or crystal lattice of the magnetic grains within the sample (magnetic fabric). Clusters of K_1 and K_3 axes define the magnetic lineation and the pole of magnetic foliations respectively (Khan 1962).

AMS measurements on standard cylindrical samples were performed with a KLY 2 bridge with a sensibility of about 5.10^{-8} SI and accuracy as low as 0.1%. At each site both the direction and the magnitude of AMS axes were measured on 8–24 standard specimens. The parameters used to define the shape of the ellipsoid are the degree of anisotropy $P = K_1/K_3$, the lineation $L = K_1/K_2$, and the foliation $F = K_2/K_3$ (Table 1; see Hrouda's review 1982). The mean AMS data for each site has been calculated using the eigenvalue decomposition on an average susceptibility tensor (Jelinek 1978). The mean directions of maximum susceptibility axes and angles between minimum susceptibility axes and the pole of systems considered (geographic, bedding, cleavage) are reported with their confidence angles (e_{ij} within the plane K_i–K_j) on the unit sphere (Table 2).

Types of magnetic fabrics. In all the studied sites, the minimum axes of susceptibility K_3 are well grouped perpendicular to the bedding plane (S_0) or to the cleavage (S_1). In only a few sites, they are distributed within a great circle which contains the poles of these two planes. In contrast, the orientation and the clustering of the maximum susceptibility axes K_1 vary and lead us to define five different types of fabrics (Fig. 4):

Intersection fabric. This fabric is characterized by $L \approx F$. K_3 corresponds either to the pole of bedding (S_0) or to the pole of the cleavage (S_1) or distributed within a great circle between the poles of these two planes. K_1 is well defined ($e_{12} < 27°$) and parallel to the intersection of bedding and cleavage (Fig. 4a).

Planar fabric. This fabric is characterized by an oblate ellipsoid with K_3 closely perpendicular to the cleavage

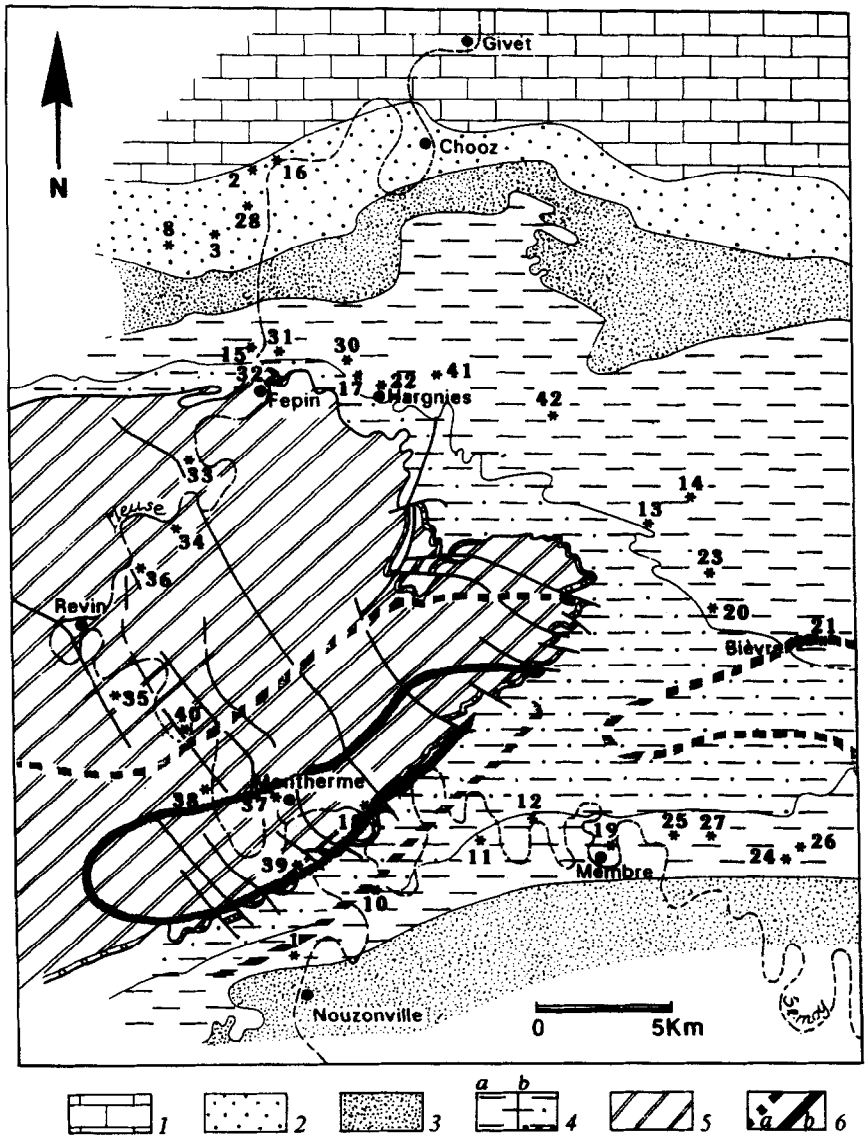

Fig. 3. Geological sketch map of the Rocroi massif with location of sites: 1—Givetian; 2—Emsian; 3—Pragien; 4a—Upper Gedinian; 4b—Lower Gedinian; 5—Cambrian; 6—(a) limit between subouter and outer metamorphic zones; (b) limit between outer metamorphic zone and inner metamorphic zone (from Beugnies 1986).

plane (in this case bedding is transposed in cleavage) and K_1 largely scattered within this plane with $e_{12} > 35°$ (Fig. 4b).

Transport fabric. This fabric exhibits a magnetic foliation parallel either to S_1 or to S_0–S_1 and a steep well-defined magnetic lineation with $e_{12} < 20°$ (Fig. 4c).

Superimposed fabric. The lineation shows two clusters running along two directions and high confidence angles $e_{12} > 20°$. One of these directions is generally parallel to the intersection between S_0–S_1 and the other is perpendicular to it (Fig. 4d).

Diffuse fabric. In this last type, the magnetic lineation remains poorly defined ($15° < e_{12} < 45°$) within the cleavage, which is parallel to bedding (Fig. 4e).

The distribution of the different types of fabrics observed in the investigated area is shown in Fig. 5. The intersection fabric is developed in the northern part of the investigated area. Superimposed fabrics are located in the North Devonian, where S_0 and S_1 are clearly distinct. When going southward, fabrics are mostly of transport, diffuse or planar types.

Evolution of anisotropy parameters

Most of the magnetic susceptibility ellipsoids determined in this study have an oblate shape with $F > L$ (Table 1). This is in agreement with the planar tectonic fabric evidenced in the field by the development of a cleavage within which the minerals do not show any clear preferential alignment. The arithmetic means of L and F parameters on each site are plotted with their standard deviation in Fig. 6. The Emsian schist are characterized by homogeneous F mean values (from 1.009 and 1.027). The L parameter remains low generally between 1.0 and 1.015.

In the Gedinnian schist, a difference is observed between north and south of the Rocroi massif with higher values of F parameter in the south. In addition, in both areas, we observe an increase of the oblate shape heading eastward. Higher values are encountered in the southeastern part of the studied area ($F = 1.5$).

The Cambrian sites show another pattern. The higher values are observed in the central part where the F and L

Table 1. Arithmetic means of anisotrophy parameters with their standard deviation *S*: $Lm = K_2/K_3$, $Fm = K_1/K_3$, Km $((K_1 + K_2 + K_3)/3)$

Site	*n*	*Lm*	*S*	*Fm*	*S*	*Km* 10–6 SI	*S*
Emsian							
2	(14)	1,0095	0,0044	1,0168	0,0175	252	81
3	(7)	1,0064	0,0026	1,0091	0,0029	139	75
8	(8)	1,0056	0,0028	1,0165	0,0099	255	56
16	(9)	1,0112	0,0034	1,0214	0,0165	296	27
28	(8)	1,0145	0,0070	1,0277	0,0184	183	35
North Gedinian							
15	(23)	1,0111	0.0060	1,0313	0,0165	351	46
31	(9)	1,0157	0,0033	1,0223	0,0072	296	27
30	(11)	1,0192	0,0089	1,0613	0,0132	339	64
17	(9)	1,0166	0,0061	1,0283	0,0057	280	39
22	(11)	1,0172	0,0057	1,0352	0,0206	217	30
42	(10)	1,0230	0,0068	1,0225	0,0136	294	79
41	(12)	1,0093	0,0060	1,0143	0,0079	343	65
20	(12)	1,0122	0,0047	1,0343	0,0076	232	30
14	(9)	1,0197	0,0070	1,0256	0,0128	241	53
13	(11)	1,0233	0,0164	1,0563	0.0209	213	47
23	(11)	1,0148	0,0048	1,0941	0,0185	192	27
21	(15)	1,0844	0,0571	1,1669	0,1195	257	121
Cambrian							
32	(10)	1,0234	0,0143	1,0663	0,0161	330	69
33	(15)	1,0247	0,0213	1,0877	0,0306	486	219
34	(9)	1,0281	0,0272	1,0940	0,0311	386	42
36	(10)	1,0517	0,0761	1,2474	0,1080	438	140
35	(13)	1,1016	0,1025	1,2126	0,1620	1090	1341
38	(11)	1,1734	0,1610	1,4730	0,2999	963	674
40	(8)	1,0107	0,0039	1,2040	0,0453	334	184
37	(12)	1,0262	0,0255	1,1944	0,1416	363	192
39	(10)	1,0076	0,0035	1,2400	0,0373	464	88
18	(13)	1,0374	0,0350	1,1949	0,0578	391	78
South Gedinian							
1	(24)	1,0261	0,0167	1,0671	0,0316	195	92
10	(9)	1,0248	0,0091	1,0570	0,0116	267	29
11	(10)	1,0094	0,0041	1,0434	0,0235	255	82
12	(12)	1,0253	0,0142	1,0711	0,0288	277	75
19	(11)	1,0409	0,0223	1,1527	0,0868	511	286
25	(9)	1,0159	0,0058	1,1390	0,0215	311	65
27	(12)	1,0408	0,0275	1,3770	0,1063	359	57
24	(9)	1,0146	0,0045	1,2029	0,0290	303	30
26	(11)	1,0357	0,0231	1,2816	0,1003	333	83

parameters reach 2.0 and 1.4 respectively (site 38). From this site a decrease of *F* and *L* parameters is evidenced northward and southward.

At the regional scale, the general tendency is a southward increase of the *F* parameter. Two specific anomalies are observed: in the Cambrian schist (peak of *F* parameter) and in the Gedinnian cover (fall of *F* parameter). The *L* parameter remains low but is higher south than north of the Rocroi massif.

Magnetic mineralogy

We have studied clay-rich rocks from three different formations that have experienced low-grade metamorphism (Beugnies 1963, 1986). It is known that various mineralogical assemblages (both in the ferromagnetic minerals and in the matrix) can produce AMS ellipsoids not simply related to the degree of deformation (Borradaile 1988). In order to precisely determine the origin of the magnetic fabric we have analyzed the magnetic mineralogy of the studied formations. We have chosen one or several samples per sites that behave as close as possible to the tensorial mean.

From thin section analysis, and according to Meilliez (1989), we know that the matrix of both Devonian and Cambrian formations is dominated by paramagnetic chlorite and muscovite. The nature of the ferromagnetic minerals is inferred from coercivity/blocking temperature spectrum analysis, based on the protocol proposed by Lowrie (1990). Samples are stepwise thermally demagnetized after saturation along their three axes successively in high (2.7 T), intermediate (0.1 T) and low (0.025 T) magnetic fields.

The Emsian schist, in the northern part of the studied area, does not show any intermediate and low coercivity components (Fig. 7a). The magnetization carried by the high coercivity component is removed at a temperature higher than 640°C indicating that hematite is the main ferromagnetic mineral in these rocks.

The magnetic mineralogy of Gedinnian sites is much more variable. In some sites situated north of the Rocroi massif, the results are about the same as in the Emsian

Table 2. Statistical parameters and type of fabric of the sampled sites. For each site parameters are determined using the decomposition on average susceptibility tensor (Jelinek 1978). n: Number of samples; Δz: angle between the mean minimum susceptibility axis and the pole of the considered system; D: mean strike of maximum susceptibility axis in the plan of the considered system; e_{12}: confidence angle between mean maximum and mean intermediate susceptibility axes

		Geograp. system		Bedd. system		Cleav. system			
Site	n	$Dz.$ (°)	$D.$ (°)	$Dz.$ (°)	$D.$ (°)	$Dz.$ (°)	$D.$ (°)	e_{12} (°)	Fabric type
Emsian									
2	(14)	44	69	16	72	10	71	19	I
3	(7)	9	73	13	253			27	I
8	(8)	75	67	13	76	35	70	23	I
16	(9)	44	66	11	68	34	246	7	I
28	(8)	6	53	6	53			15	I
North Gedinian									
15	(23)	9	53	20	233	15	54	34	S
31	(9)	13	210	13	210	37	213	19	I
30	(11)	14	355	10	176	23	0	61	S
17	(9)	29	161	35	169	10	338	9	T
22	(11)	13	212	40	216	16	212	40	S
42	(10)	45	77	70	259	21	257	29	S
41	(12)	31	62	11	242	11	242	21	S
20	(12)	52	105	58	101	15	292	36	P
14	(9)	23	98			23	282	19	D
13	(11)	26	138			10	317	23	D
23	(11)	33	83			20	259	53	P
21	(15)	31	155	27	159	1	155	10	T
Cambrian									
32	(10)	31	126	21	307	4	310	39	D
33	(15)	27	136	4	138	18	319	19	T
34	(9)	44	262	22	77	6	254	37	P
36	(10)	28	191	7	10	19	9	23	D
35	(13)	27	157			13	338	36	D
38	(11)	22	176	7	354	11	355	14	T
40	(8)	23	202	23	202	18	22	58	T
37	(12)	30	170	12	350	9	350	51	P
39	(10)	31	196	8	16	24	15	25	D
18	(12)	21	177	3	355	7	357	14	T
South Gedinian									
1	(24)	58	153			4	156	16	D
10	(9)	50	228	50	228	6	217	17	D
11	(10)	38	187	5	196	6	2	23	D
12	(12)	49	96			8	104	75	P
19	(11)	51	245			12	236	22	D
25	(9)	41	193	44	190	12	6		D
27	(12)	38	187	7	184	16	4	14	T
24	(9)	38	168	15	349	10	350	40	D
26	(11)	27	163	5	344	22	343	15	T

schist with hematite as the main magnetic carrier (Fig. 7b). However the diagrams are generally more complex. The coercivity spectra are very large and different blocking temperature are observed. Goethite (high coercivity, unblocking temperature around 120°C), magnetite and hematite occur in variable quantities (Fig. 7c). The contribution of additional low to intermediate coercivity components is removed at temperatures varying between 350 and 380°C (Fig. 7c) and a value higher than 640°C (Fig. 7d). The unblocking temperature of about 350°C would suggest the presence of either iron sulphides or maghemite. Maghemite seems more realistic because in the same specimen we also found hematite which represents an oxidized phase. In the same way, the low and intermediate coercivity/high unblocking temperature component (Fig. 7d) may be carried by acicular single domain maghemite (Özdemir & Banerjee 1984), although such high blocking temperature has not been recognized in natural maghemite.

The Cambrian schist show a large occurrence of magnetite around the Rocroi massif (Fig. 7e) and pyrrhotite (Fig. 7f), in the central part, detected by the maximum blocking temperature of 580°C and 340°C, respectively. Pyrrhotite (confirmed by X-ray analyses) is clearly of metamorphic origin and likely derived from the pyrite of sedimentary origin described in this region (Beugnies 1963, Fourmarier *et al.* 1968, Beugnies 1986).

In summary, in the Gedinnian Formation, hematite, probably maghemite and magnetite (in the south) are the principal ferromagnetic grains whereas magnetite and pyrrhotite are dominant in the Cambrian (Fig. 8).

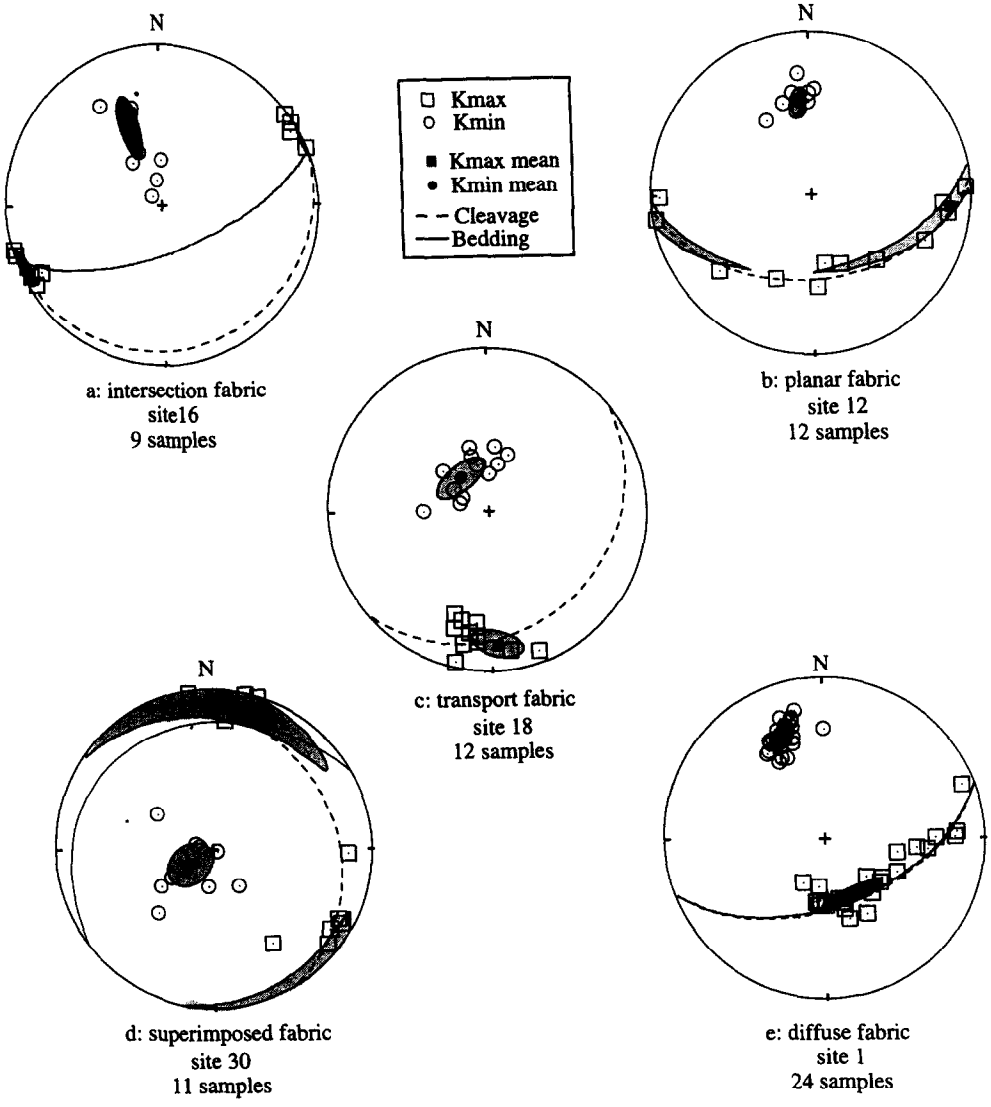

Fig. 4. Typical examples of the different types of magnetic fabrics observed in the studied area with their confidence ellipses (dashed zones). (a) Intersection fabric; (b) planar fabric; (c) transport fabric; (d) superimposed fabric; (e) diffuse fabric.

DISCUSSION

The main aim of this paper is to determine the effects of the magnetic mineralogy on the bulk magnetic fabric. This requires discussion on two major points: (1) the origin of the magnetic mineralogy and its relationship to metamorphism; and (2) the relationships between magnitude and direction of AMS axes and magnetic mineralogy. After examining the role of magnetic mineralogy, we will interpret the AMS data in a tectonic framework.

Relationships between metamorphism and magnetic mineralogy

Ferromagnetic mineralogy complements the metamorphic zonation established by Beugnies (1963, 1986, Fig. 8). Three mineralogical transformations, roughly corresponding to isograde defined by this author, are found:

(1) The development of pyrrhotite in the Cambrian schist may be linked to the metamorphism, by breakdown of pyrite (Hall 1986, Rochette & Lamarche 1986) which could outline the 300°C isotherm.

(2) The occurrence of magnetite in the South Cambrian and South Gedinnian probably delimits the breakdown of pyrrhotite into magnetite (Bina *et al.* 1991) at 500°C, which has been already outlined by Beugnies (1986).

(3) If our suggestion that maghemite is one of the ferromagnetic minerals in the Gedinnian sites is true, we observe that the occurrence of this mineral is associated with relatively high-grade metamorphism. We observe the change of low-temperature to high-temperature maghemite along a W–E transept in the Gedinnian cover (Fig. 7). This kind of variation has not yet been discussed in literature and remains quite difficult to interpret.

Thus, in the Ardennes rocks, the ferromagnetic mineralogy in mainly controlled by metamorphism. The two anomalies in the F distribution, peak of F parameter in Cambrian schist and fall of F parameter in the Gedinnian cover, are controlled by changes in magnetic miner-

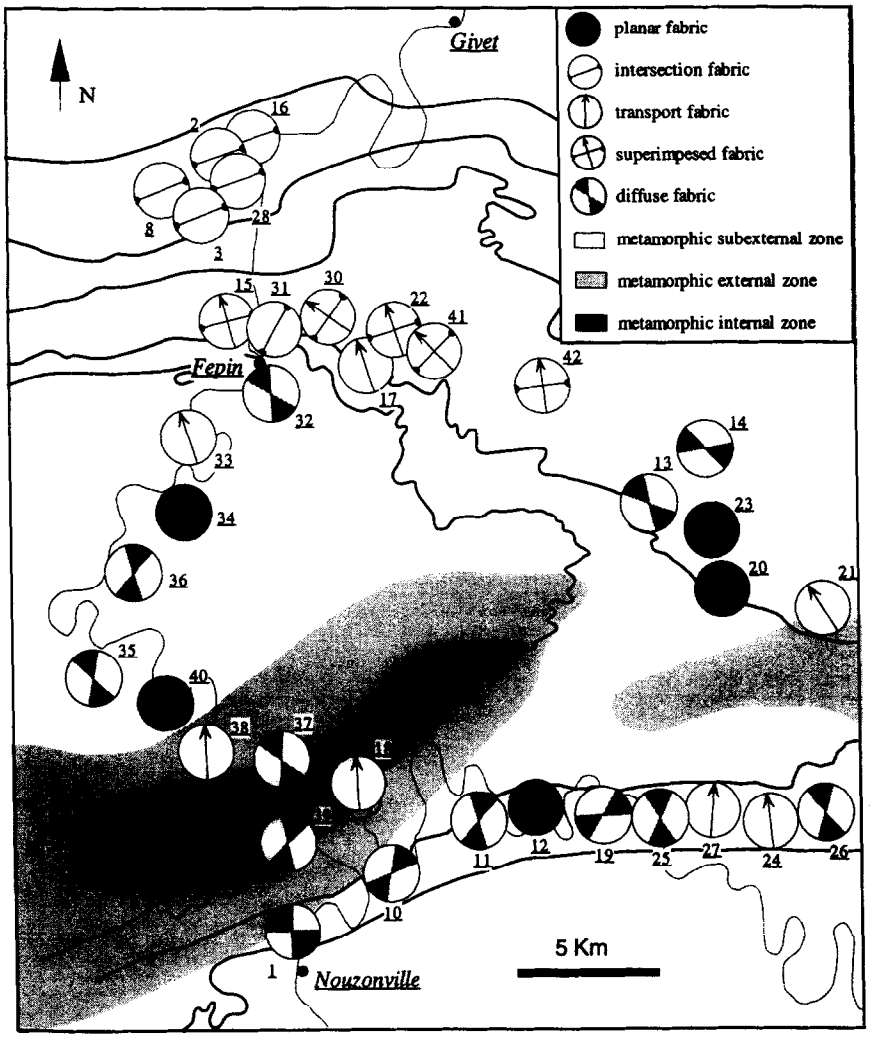

Fig. 5. Distribution of the magnetic fabrics in the Rocroi massif (see also Fig. 4). The metamorphic zones are from Beugnies (1986).

alogy; the occurrence of pyrrhotite and the occurrence of a particular paragenesis (magnetite + maghemite (?) + hematite), respectively.

Relationships between magnetic fabric and magnetic mineralogy

Mineralogical control of magnitude of AMS axes. It is well known that the growth of new minerals or the existence of multiple and variable sources of susceptibility invalidate the use of *L–F* parameters to determine the strain intensity (Borradaile 1987, Rochette 1988). This is particularly obvious in the studied region where multiple mineralogical transformations have occurred.

For a rock containing pyrrhotite or magnetite, Rochette *et al.* (1992) proposed a limit between 350.10^{-6} and 500.10^{-6} SI above which the ferromagnetic minerals carry susceptibility and below which both the ferromagnetic fraction and the matrix term affect the susceptibility and its anisotropy. In our samples, *Km* extends from 90.10^{-6} SI to 5000.10^{-6} SI, and a graph of *P* vs *Km* appears to be an appropriate tool for determining variations of *P* related to changes in the magnetic mineralogy independent from strain variations.

In Emsian and north Gedinnian Formations, characterized by the same magnetic mineralogy, *P* varies from 1.002 to 1.15 and *Km* from 90.10^{-6} SI to 450.10^{-6} SI without any clear correlation (Fig. 9a). The lowest *P* values observed in the Emsian Formation are probably due to the abundance of quartz in this formation. The lack of correlation between *P* and *Km* may reflect the abundance of a mineral with either low intrinsic *P* values or low preferential orientation. As the ferromagnetic phase detected in this zone is mainly hematite, which presents intrinsic properties higher than any paramagnetic phase (intrinsic anisotropy up to 100), we interpret the low *P* values as the result of a low preferred orientation of hematite crystallographic axes (Borradaile 1988).

In the South Gedinnian Formation large *P* values (up to 1.6) are associated to large values of $Km > 350.10^{-6}$ SI (Fig. 9b). This illustrates the relative increase of the contribution of hematite and high temperature maghemite (with closed symbols on Fig. 9b) to the AMS. In this case the degree of anisotropy is thus mainly controlled by changes in the magnetic mineralogy.

Most of the samples from the central part of the Rocroi massif (Cambrian), where pyrrhotite has been

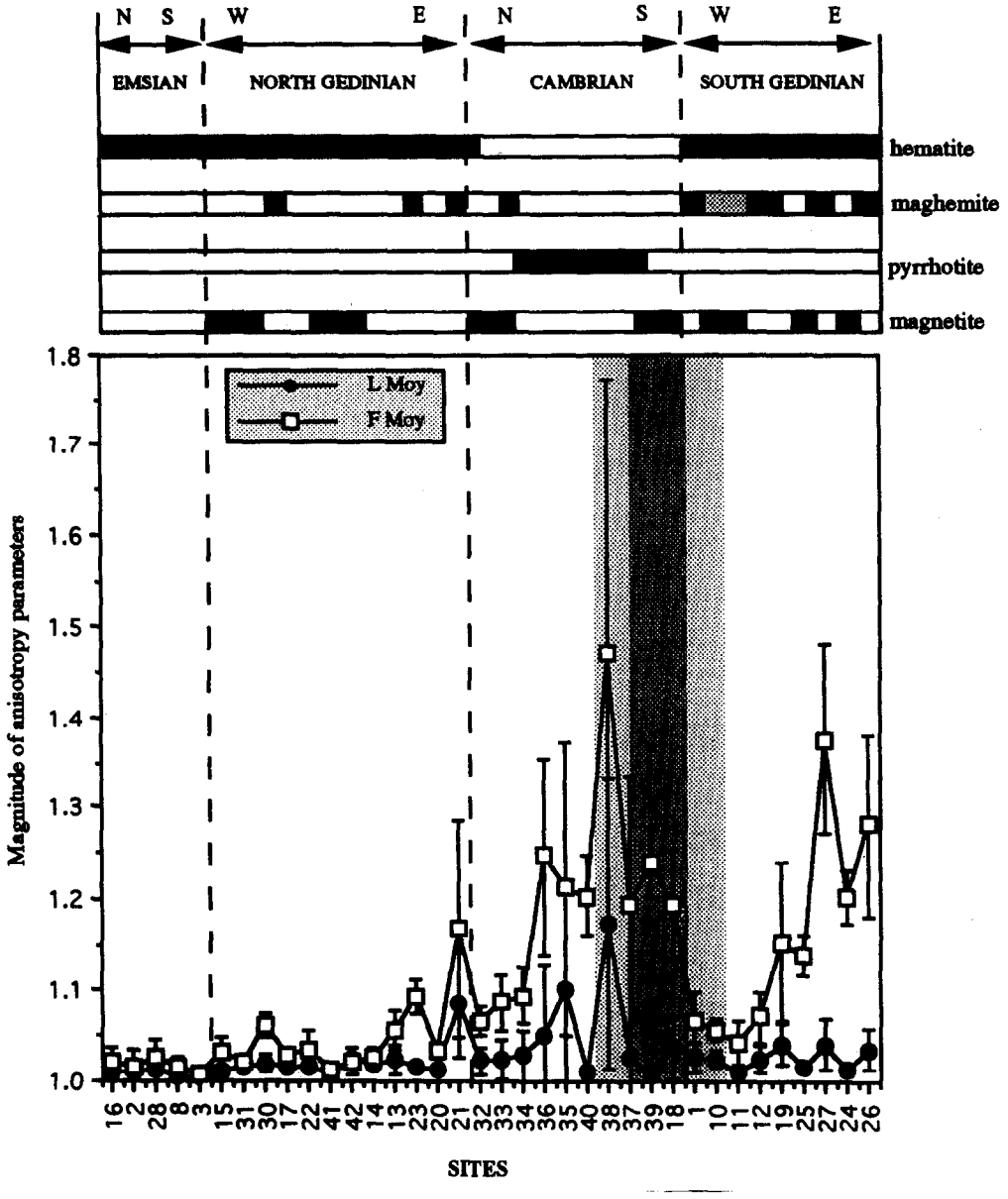

Fig. 6. Distribution of the mineralogical phases and the evolution of L (K_1/K_2) and F (K_2/K_3) anisotrophy parameters vs geographic location. L and F values are calculated using arithmetic means their standard deviation is reported. The dashed areas locate the metamorphic internal (black) and external (clear) zones (Beugnies 1986). Also indicated in block area the magnetic mineralogy. Dashed zone corresponds to occurrence of maghemite with low inverted temperature (see text).

identified, show an increase of P vs Km for $Km > 500.10^{-6}$ SI and $P > 1.30$ (Fig. 9c). This is related to the development of pyrrhotite which exhibits very high intrinsic magnetocrystalline anisotropy (Pi up to 1000). Samples from the periphery of the Rocroi massif with magnetite as the dominant ferromagnetic phase, show subtle positive correlation. P is generally lower than 1.35 and Km ranges between 200.10^{-6} SI and 600.10^{-6} SI. Consequently, matrix and ferromagnetic phases both contribute to low field susceptibility and anisotropy in the Cambrian schist.

Mineralogical control of the direction of magnetic lineation. The intersection fabric is observed in the north of the studied area where anisotropy is governed by planar minerals such as hematite and phyllosilicates. Intersection fabrics in such rocks are generally considered as the result of heterogeneous combinations of subfabrics (Borradaile 1988) or composite fabrics (Housen *et al.* 1993). The magnetic lineation marks the zonal axis about which the basal plane of the minerals are disposed partly along the cleavage and partly along the bedding. This can result from pressure-solution processes leading to a concentration and a mechanical reorientation of phyllosilicates and hematite and likely growth of these same phases along the cleavage.

The transport fabric appears associated with the occurrence of pyrrhotite or magnetite (Cambrian schist and southwestern part of Gedinnian cover). It is also particularly well expressed in the zone where possible maghemite (?) has been observed (southeastern part of Gedinnian). Pyrrhotite and magnetite, contrary to phyllosilicates and hematite, are known to have significant intrinsic linear anisotropy (Rochette 1988). This mag-

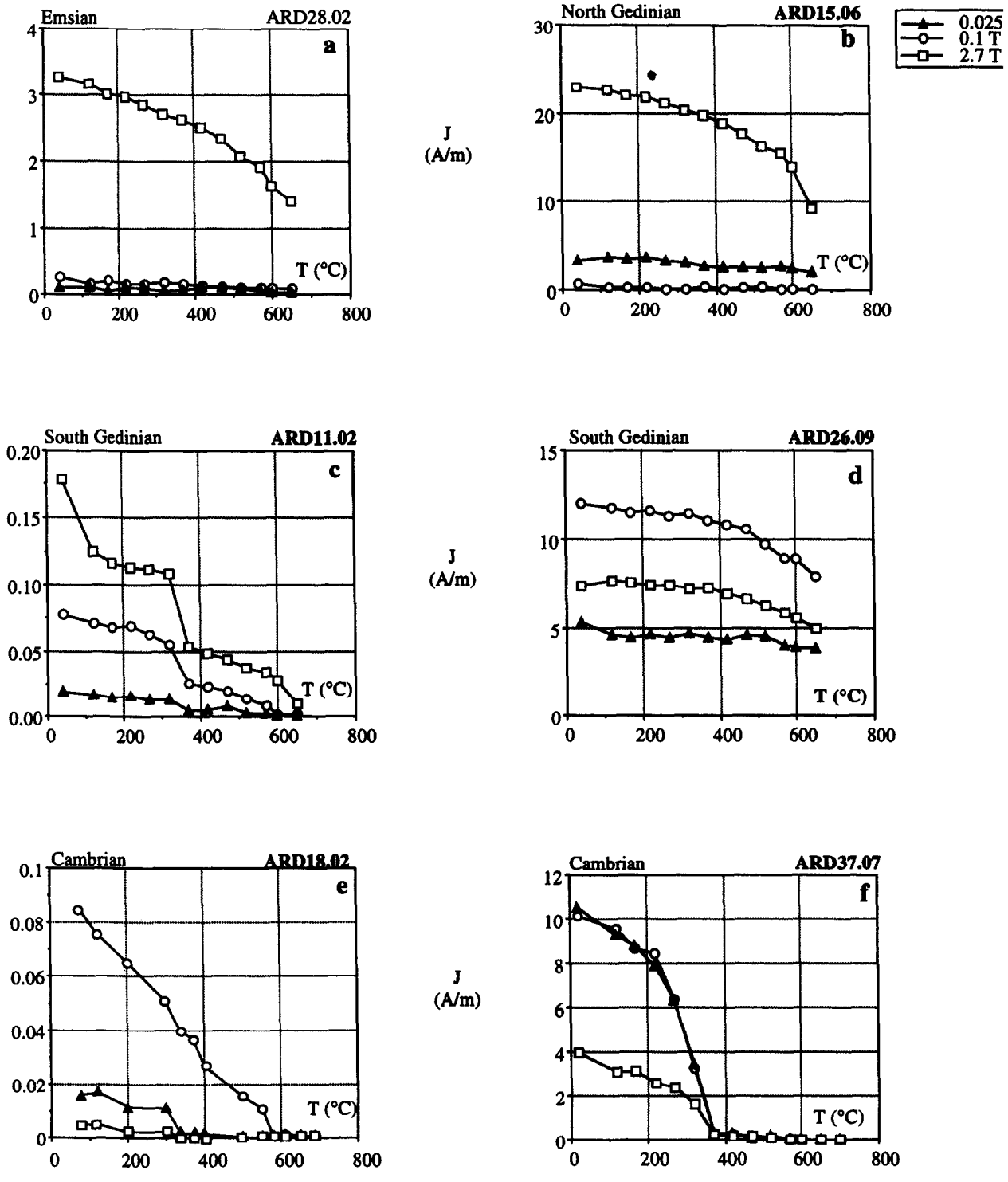

Fig. 7. Blocking temperature spectra of three isothermal remanent magnetizations of 0.025 T (closed triangle), 0.1 T (open circle), 2.7 T (open square). (a) Typical Emsian sample; (b) typical North Gedinian sample; (c) typical southwest Gedinian sample; (d) typical southeast Gedinian sample; (e) sample from periphery of Cambrian; (f) sample from the central part of Cambrian.

netic lineation results either from crystallographic alignment of grains formed as a new phase within the cleavage (pyrrhotite) or from grouping of grains forming elongated masses (magnetite) observed in thin sections. The existence of an intrinsic linear anisotropy in maghemite has not been mentioned in literature. Nevertheless appearance of high inverted temperature maghemite is associated with the increase of L parameter and the existence of transport fabrics. In all cases, the lineation which marks the maximum extension undergone by the studied rocks is associated with minerals formed during the metamorphic event. Thus deformation and metamorphism occurred synchronously.

The superimposed fabric is developed in the transition zone between the domains where intersection and transport fabrics are expressed (Fig. 5). In this zone the magnetic mineralogy is not homogenous (Fig. 8) and varies from sample to sample. Referring to the above discussion, we suggest that intersection fabric persists in samples where planar minerals remain dominant,

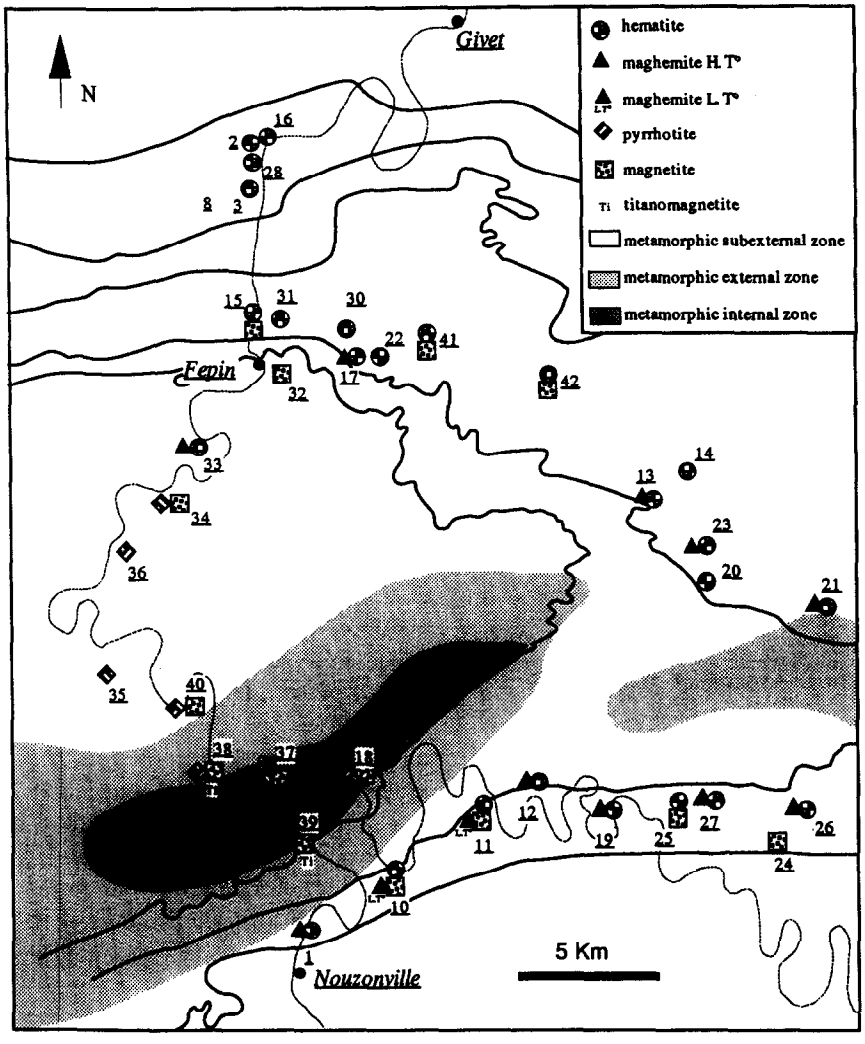

Fig. 8. Distribution of the magnetic mineralogy in the Rocroi massif (see also Fig. 6). The metamorphic zones are from Beugnies (1986).

whereas transport fabric reveals samples containing magnetite. If this hypothesis is true, superimposed fabric should be an illustration of incomplete metamorphic transformations.

The diffuse and planar fabrics, in which no clear lineations are observed, are developed in the southern part of the studied area (i.e. in the zone where transport fabric is also observed). No clear progressive transition from one type to another can be inferred from the map pattern (Fig. 5). However, this zone is precisely the domain where the post-kinematic dome described by Beugnies (1986) is developed. Consequently, we interpret the diffuse and planar fabrics as the result of post-kinematic alterations of previous transport fabrics. Such phenomena could be due to the growth of new mineralogical phases within the cleavage but without preferential orientation within this plane. On the basis of geological observations this fact was already established by Fourmarier *et al.* (1968) around the localities of Louette St Pierre (sites 13, 20) and Vresse (site 19), and more generally in the eastern part of the studied area. Our results support these field observations.

In summary, the mineralogical control of these types of fabric seems clear:

(1) phyllosilicate and hematite are associated with intersection lineation;

(2) pyrrhotite, magnetite and the phase interpreted as maghemite, more likely record the transport direction;

(3) occurrence of multiple contrasting magnetic carriers or post-tectonic minerals could lead to undefined magnetic lineation (diffuse and planar fabrics).

Tectonic interpretation: evidence for a change in the tectonic transport direction

We have shown that the different types of fabrics could be controlled by the mineralogical assemblages. However, the ones in which the transport direction is visible are independent from the formation (Devonian as well as Cambrian), from the magnetic mineralogy (it appears in magnetite or pyrrhotite bearing rocks) and from the metamorphic grade (it passes through the zones defined by Beugnies 1986).

The transport lineation measured in numerous sites (Fig. 5), exhibits a change in direction, from north–south in southern part of the study area to northwest–southeast in the northern part. The lineation is normal to

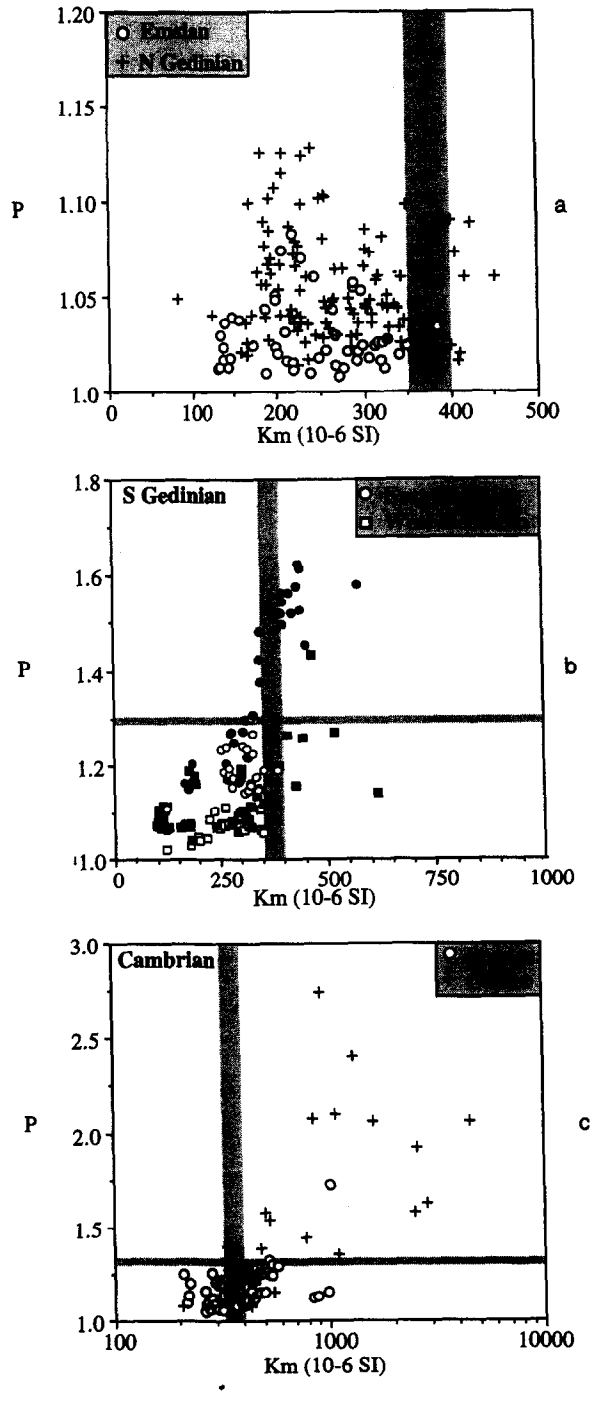

Fig. 9. $P(K_1/K_3)$ vs Km ($Km = (K_1 + K_2 + K_3)/3$) in the studied area. (a) White dots: Emsian sites (2, 3, 8, 16, 28); cross: north Gedinian sites (13 to 15, 17, 20, 22, 23, 30, 31). (b) Circles: southwest Gedinian sites (1, 10, 11, 12, 19); squares: southeast Gedinian sites (21, 24, 25, 26, 27); the black points are these with supposed high temperature maghemite. (c) Circles: periphery of Cambrian sites (32, 33, 18, 37, 39); cross: central part of Cambrian sites (34 to 36, 38, 40). Limits for susceptibility range 350–400.10^{-6} and anisotrophy parameter $p = 1.3$ are dashed.

the intersection lineation observed on the same sites or on sites where the intersection fabric is the only one present.

The tectonic origin of this lineation is most likely related to the direction of shearing (northward or northwestward) due to the nappe transport. From this point of view, our work gives an important set of new data which complete and improved previous kinematic data (Meilliez 1984). In particular, the change in shearing direction from the south to the north of the Rocroi massif had not been documented previously and recent kinematics syntheses (Hugon 1982, Rathore & Hugon 1987, Le Gall 1992) considered generally a bulk and unique northward or north-northwestward tectonic transport. It is worth noting that the two directions are normal to the two regional trends of the major structures observed at the scale of the Variscan front (Fig. 1).

The orientation of the lineation is independent from the position of sites below or above the Ardennes unconformity. Two tectonic consequences can be inferred from this: (i) the strain observed in the Cambrian massif and in the overlying Devonian cover is only due to Variscan orogeny; (ii) the late thrust faults cutting through the orogenic wedge (Fig. 2) did not lead to significant differential rotations between the different thrust sheets.

Concerning the regional significance of the apparent change in the tectonic transport direction, three main tectonic hypotheses can be considered to explain the observed pattern (Fig. 10).

(i) In the first hypothesis the apparent change resulted from the superposition of two tectonic events characterized by different tectonic transport directions. In the northern part of the studied area the fold-and-thrust system clearly results from a progressive deformation characterized by a unique tectonic transport normal to the fold axes and to the magnetic lineation (i.e. northwestward). Consequently, if this hypothesis of superimposition is true, it would have affected only the southern part of the studied area where the development of a late N-verging event would have overprinted the first NW-verging one. The structural evidence does not support the existence of these two transport directions. On the other hand, such a tectonic scenario is inconsistent with chronological data showing that the thrust sequence and related deformation are globally forward developing (Piqué *et al.* 1984).

(ii) In the second hypothesis the apparent change would have resulted from late differential rigid body rotation between the northern and southern parts of the area. This hypothesis is plausible and even demonstrated in other sectors of the Variscan belt (Thominski *et al.* 1993). Edel & Coulon (1986) suggested a post-Variscan clockwise rotation of the whole Ardennes massif. However, a differential rotation requires a decoupling zone along which the rotation occurred. This decoupling zone should be expressed in the Rocroi massif as a major fault zone (either a thrust-fault or a strike-slip fault). Detailed geological mapping (Beugnies 1963, Meilliez 1991) does not support such an hypothesis.

(iii) In the third hypothesis the change is due to a progressive variation of shearing direction during the forward propagation of the thrust system. Using various incremental strain measurements, Dittmar *et al.* (1994) discuss a similar anticlockwise rotation of the principal direction of shortening in the Rhenish massif, 150 km east of the studied area. They presume that the orogenic wedge evolved through several stages of non-homoaxial

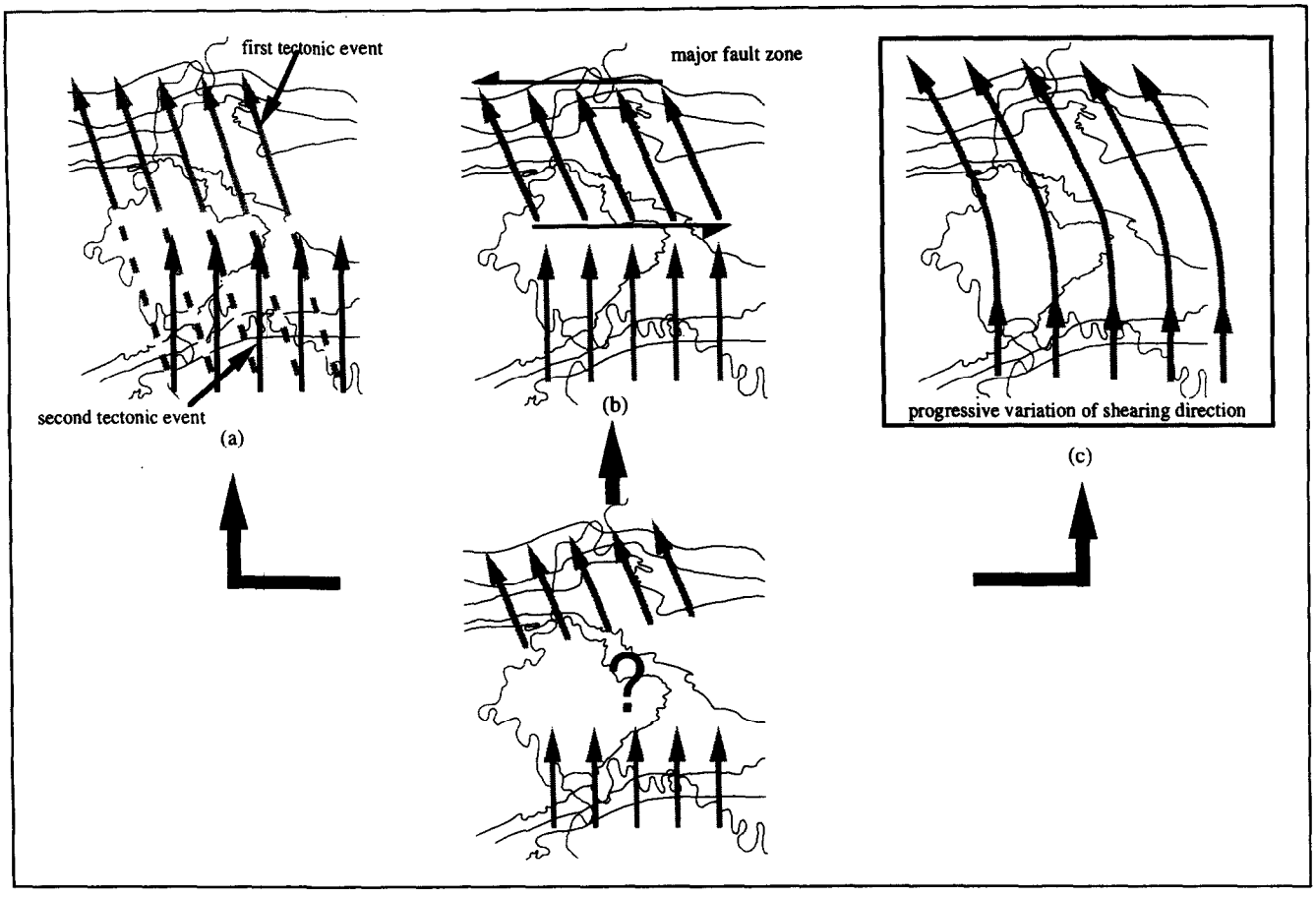

Fig. 10. Three main tectonic hypotheses to explain the magnetic fabric pattern in and around the Rocroi massif. (a) Superposition of two tectonic events characterized by different transport directions; (b) differential rigid body rotation linked, for instance to a strike-slip faults acting as a decoupling zone; (c) variation of shearing direction during the forward propagation of the thrust system.

deformation increments. Accordingly, our data support this hypothesis of a progressive bend of the transport direction during the propagation of the wedge.

CONCLUSIONS

This study in and around the Rocroi massif gives a set of new data about the structural evolution of the Ardennes Thrust-Belt. In particular, the magnetic mineralogy, directly controlled by the metamorphism, provides new isograds (isograd pyrrhotite +, isograd pyrrhotite − and potentially isograds maghemite ±) and therefore new constraints on the metamorphic pattern. However further work is needed to complete the mapping of changes in magnetic mineralogy.

The influence of magnetic mineralogy on the magnitude of AMS axes is shown. The types of fabric depend on both the mineralogy and the structural position of sites. In particular, diffuse and planar fabrics seem connected to the development of post-kinematics minerals within the cleavage plane. Despite these difficulties, we establish that the direction of AMS axes are independent from the stratigraphic level and from the metamorphic grade. It is of tectonic origin and leads us to document a change of about 25° (from N–S to NNW–SSE) in the shearing direction of the nappe pile. It appears that AMS measurements give useful kinematic data as relative strain gauges in regions where mineralogical changes occurred.

Acknowledgements—The authors wish to thank G. Roche (CNRS, URA 1369) for some drawings, F. Bejina for his active help in the field and J. Marcus for improving the English. Helpful comments by R. Van der Pluijm, J. P. Evans and an anonymous reviewer are gratefully acknowledged. This is a C.F.R. contribution, no. 1677.

REFERENCES

Aubourg, C., Rochette, P. & Vialon, P. 1991. Subtle stretching lineation revealed by magnetic fabric of Callovian–Oxfordian black shale (French Alpes). *Tectonophysics* **185**, 211–223.

Averbuch, O., Frizon de Lamotte, D. & Kissel, C. 1992. Magnetic fabric as a structural indicator of the deformation path within a fold-thrust structure: a test case from the Corbières (NE Pyrenees France). *J. Struct. Geol.* **14**, 461–474.

Averbuch, O., Frizon de Lamotte, D. & Kissel, C. 1993. Strain distribution above a lateral culmination: an analysis using microfaults and magnetic fabric measurements in the Corbières thrust belt (NE Pyrenees, France). *Annls Tectonicae* **VII**, 3–21.

Beugnies, A. 1963. Le Massif Cambrien de Rocroi. *Bull. Serv. Carte géol. Fr.* **270**, 117–121.

Beugnies, A. 1986. Le métamorphisme de l'aire anticlinale de l'Ardenne. *Hercynica* **II**, 17–33.

Bina, M., Corpel, J., Daly, L. & Debeglia, N. 1991. Transformation de la pyrrhotite sous l'effet de la temperature: une source d'anomalies magnétiques. *C. r. Acad. Sci., Paris* **313**, 487–494.

Borradaile, G. 1987. Anisotropy of magnetic susceptibility: rock composition versus strain. *Tectonophysics* **138**, 327–329.

Borradaile, G. J. 1988. Magnetic susceptibility, petrofabric and strain. *Tectonophysics* **156**, 1–20.

Bouroz, A. 1950. Sur quelques aspects du mécanisme de la déformation tectonique dans le bassin houiller du Nord de la France. *Annls Soc. géol. N.* **LXX**, 1–23.

Cazes, M., Torreilles, G., Bois, C., Damotte, B. Galdéano, A., Hirn, A., Mascle, A., Matte, P., Pham, V. N. & Raoult, J.-F. 1985. Structure de la croûte hercynienne du Nord de la France: premiers résultats du profil ECORS. *Bull. Soc. geol. Fr.* **8**, 925–941.

Delvaux de Fenffe, D. & Laduron, D. 1984. Analyse structurale au bord sud du massif de Rocroi (Ardennes françaises). *Bull. Soc. géol. Bel.* **T.93**, 11–26.

Dittmar, D., Meyer, W., Oncken, O., Walter, S. Th. R. & Winterfeld, R. 1994. Strain partitioning across a fold and thrust belt: the Renish Massif, Mid-European Variscide. *J. Struct. Geol.* **16**, 1335–1352.

Edel, J.-B. & Coulon, M. 1986. Mise en évidence de rotations tardihercyniennes à partir d'un profil paléomagnétique à travers l'Ardennes et le Brabant. *Annls Soc. géol. N.* **CV**, 139–144.

Fourmarier, P. 1913. Les phénomènes de charriage dans le bassin de Sambre-Meuse et le prolongement du terrain houiller sous la Faille du Midi dans le Hainaut. *Bull. Soc. géol. Belg.* **40**, 192–235.

Fourmarier, P., Bintz, J. & Lambrecht, L. 1968. Anomalies de la schistosité dans le paléozoïque de la haute-Ardennes. *Annls Soc. géol. Belg.* **91**, 171–269.

Hall, A. J. 1986. Pyrite–pyrrhotine redox reactions in nature. *Mineralog. Mag.* **50**, 223–229.

Housen, B. A., Richter, C. & Van der Pluijm, B. A. 1993. Composite magnetic anisotrophy fabrics: experiments, numerical models, and implication for quantification of rocks fabrics. *Tectonophysics* **220**, 1–12.

Housen, B. A. & Van de Pluijm, B. A. 1991. Slaty cleavage development and magnetic anisotropy fabrics. *J. geophys. Res.* **96**, 9937–9946.

Hrouda, F. 1982. Magnetic anisotrophy of rocks and its applications in geology and geophysics. *Geophys. Surv.* **5**, 37–82.

Hugon, H. 1982. Structure et déformation du massif de Rocroi (Ardennes). Approche géométrique, quantitative et expérimentale. Thesis of 3iem cycle, University of Rennes, Rennes, France.

Jelinek, V. 1978. Statistical processing of anisotrophy of magnetic susceptibility measured on groups of specimens. *Studia Geoph. & Geod.* **22**, 50–62.

Kaisin, F. 1936. Le problème tectonique de l'ardenne. Thesis, University of Louvain.

Khan, M. A. 1962. The anisotrophy of magnetic susceptibility of some igneous and metamorphics rocks. *J. geophys. Res.* **67**, 2863–2885.

Kissel, C., Barrier, E., Laj, C. & Lei, T.-Q. 1986. Magnetic fabric in 'undeformed' marine clays from compressional zones. *Tectonics* **5**, 790–781.

Le Gall, B. 1992. The deep structure of the Ardennes Variscan thrust belt from structural and ECORS seismic data. *J. Struct. Geol.* **14**, 431–546.

Lee, T.-Q., Kissel, C., Laj, C., Horng, C.-S. & Lue, Y.-T. 1990. Magnetic fabric analysis of Plio-Pleistocene sedimentary formation of coastal range of Taiwan. *Earth Planet. Sci. Lett.* **98**, 23–32.

Lowrie, W. 1990. Identification of ferromagnetic minerals in rock by coercivity and unblocking temperature properties. *Geophys. Res. Lett.* **17**, 159–162.

Meilliez, F. 1984. La formation de Fépin (Gédinnien de l'Ardenne): un marqueur régional lithostratigraphique et structural. *Annls Soc. géol. N.* **CIII**, 37–53.

Meilliez, F. 1989. Tectonique distensive et sédimentation à la base du Devonien, en bordure NE du Massif Rocroi (Ardennes). *Annls Soc. géol. N.* **CVII**, 281–295.

Meilliez, F. 1991. Ardennes–Brabant. *Bull. Sci. Geol.* **44**, 3–29.

Meilliez, F. Fiellitz, W., Laduron, D., Mansy, J.-L. & Manby, G. 1994. The deep structure of the Ardennes Variscan thrust belt from structural and ECORS seismic data: discussion. *J. Struct. Geol.* **16**, 431–432.

Meilliez, F. & Mansy, J.-L. 1990. Déformation pelliculaire différenciée dans une série lithologique hétérogène: le Dévono-Carbonifère de l'Ardenne. *Bull. Soc. geol. Fr.* **8**, 177–188.

Özdemir, O. & Banerjee, S. K. 1984. High temperature stability of maghemite. *Geophys. Res. Lett.* **11**, 161–164.

Piqué, A., Huon, S. & Clauer, N. 1984. La schistosité hercynienne et le métamorphisme associé dans la vallée de la Meuse, entre Charleville-Mezières et Namur (Ardennes Franco-Belges).

Raoult, J.-F. 1988. Le front Varisque du Nord de la France: interprétation des principales coupes d'après les profils sismiques, le géologie de surface et les sondages. In: *Etude de la croûte terrestre par sismique profonde. Profil du nord de la France.* Technip, Paris, 171–196.

Rathore, J. S. & Hugon, H. 1987. Comparison of magnetic, mica and reduction spot fabric in the Rocroi massif–Ardennes, France. In: *The Renish Massif* (edited by Vogel, A., Miller, H. & Greilling, R.). F. Vieweg and Sohn, Brauschweig/Weisbaden, 79–94.

Rochette, P. 1988. Relation entre déformation et métamorphism alpin dans les schistes noirs helvétiques: l'apport de la fabrique magnétique. *Geodyn. Acta* **2**, 17–24.

Rochette, P., Jackson, M. & Aubourg, C. 1992. Rock magnetism and interpretation of anisotrophy of magnetic susceptibility. *Rev. Geophys.* **30**, 209–226.

Rochette, P. & Lamarche, G. 1986. Evolution des propriétés magnétiques lors de transformation dans les roches: exemple du Jurassique Dauphinois (Alpes Française). *Bull. Mineral.* **109**, 687–696.

Tarling, D. H. & Hrouda, F. 1993. *The Magnetic Anisotropy of Rocks.* Chapman & Hall, 212 pp.

Thominski, H. P., Wohlenberg, J. & Bleil, U. 1993. The remagnetization of Devono-Carboniferous sediments from the Ardenno-Rhenish Massif. *Tectonophysics* **225**, 411–431.

Waterlot, G. 1937. Structure du Massif cambrien de Rocroi. *C. r. Acad. Sci. Paris* **204**, 139.